Eur. Phys. J. D **38**, 265–276 (2006)
DOI: 10.1140/epjd/e2006-00025-3

THE EUROPEAN PHYSICAL JOURNAL D

Energy levels and spectral lines of Ne VII*

A.E. Kramida[1,a] and M.-C. Buchet-Poulizac[2]

[1] National Institute of Standards and Technology, Gaithersburg, Maryland, 20899-8422, USA
[2] Laboratoire de Spectrométrie Ionique et Moléculaire, UMR CNRS no. 5579, Université Claude Bernard Lyon 1, Campus de la Doua, 69622 Villeurbanne Cedex, France

Received 23 September 2005 / Received in final form 28 November 2005
Published online 8 February 2006 –

Abstract. All experimental data on Ne VII, including previously unpublished beam-foil spectroscopy data, have been compiled and critically evaluated. More than a hundred spectral lines have been newly identified. For 40 transitions, the previous identifications have been revised. These revisions resolved all existing contradictions between previously published interpretations of the spectrum. An optimized level scheme has been derived from the total list of observed lines. About a hundred new energy levels have been found, including several highly excited hydrogenic levels. Based on these newly determined levels, as well as on the analysis of theoretical data, the ionization potential has been newly determined with improved confidence.

PACS. 32.10.Fn Fine and hyperfine structure – 32.10.Hq Ionization potentials, electron affinities – 32.30.Jc Visible and ultraviolet spectra – 31.15.Ct Semi-empirical and empirical calculations (differential overlap, Hückel, PPP methods, etc.)

1 Introduction

Six times ionized neon, Ne VII, belongs to the Be I isoelectronic sequence. Its ground state is $1s^2 2s^2$. This spectrum was observed and analyzed by many research teams using a wide variety of light sources. Table 1 lists the light sources and spectroscopic techniques used to observe different parts of the spectrum. The first observation of the resonance lines of Ne VII was made by Fawcett et al. [1,2] using a high-temperature discharge in neon-doped deuterium. A number of studies utilizing different types of toroidal discharge installations [3–8] significantly extended the knowledge of the energy structure and identified a large number of spectral lines belonging to this spectrum in various regions spanning from soft X-rays to the visible. The introduction of the method of excitation of energetic ionic beams by passage through a foil or gas target (commonly referred to as beam-foil technique) led to a number of new advances in the investigation of Ne VII [9–31]. A complementary means of investigation of the structure of highly-excited levels and other properties of Ne VII was provided by Auger electron spectroscopy [26,27,32–37]. Electron-beam ion traps [EBITs] made it possible to observe the X-ray spectrum of dielectronic recombination [38]. Apart from producing highly charged ions trapped in an electron beam, EBITs can also produce outgoing ionic beams. Such beams were recently employed to directly measure the energy structure of moderately excited non-autoionizing levels of Ne VII by studying the process of single-electron capture from a He gas target [39].

The importance of the Ne VII spectrum is mainly due to its presence in the solar spectrum [40,41] and the spectra of stars [42] and galactic nuclei [43]. It is also important for thermonuclear fusion research, as neon is often added to high-temperature fusion plasmas in order to stabilize them.

The Ne VII spectrum is divided into several distinct regions: soft X-ray (13–14 Å), extreme ultraviolet (65–142 Å, 200–410 Å, 465–564 Å), vacuum ultraviolet (750–1000 Å, 1100–1500 Å, and 1980–2000 Å), ultraviolet (2100–3000 Å), and visible (3000–4600 Å). Each region comprises lines belonging to transitions between certain groups of energy levels. This wide spread of the spectrum accounts for the fact that its studies are very fragmentary. This is illustrated in Table 1. Each research group focused on studying a limited wavelength range, often without trying to reconcile their line identifications with those made by other research teams. This led to a number of contradictions in the interpretation of the observed lines. Previous compilations of this spectrum, the most popular of which was done by Kelly [44], did not resolve these contradictions. Inconsistencies in existing line identifications were addressed and partially resolved by several groups of authors [21,29,31]. However, the recent beam-foil studies of Ne VII [29–31] added a number of new incompatible line identifications. In addition, interpretation of the observed X-ray lines originating from autoionizing core-excited

* Supplementary tables and sections are only available in electronic from at `http://www.eurphysj.org`.

[a] e-mail: `alexander.kramida@nist.gov`

Table 1. Light sources and techniques used to observe Ne VII transitions.

Optical spectroscopy				
Spectral range	Transitions	Light sources	Number of papers	Years
X-rays	$1s^2 2l2l' – 1s2l2l'2l''$	Ion beams: Collisions	4	1974–1983
		EBIT: Dielectronic recombinaison	1	2001
EUV	$1s^2 2l2l' – 1s^2 2l''nl'''(n = 3–6)$	Fusion plasmas	8	1961–1972
	$1s2l2l'2l''\ ^5\mathrm{L} – 1s2l2l'nl'''\ ^5\mathrm{L}'$ $(n = 3, 4)$	Ion beams: Beam-foil	11	1972–2000
VUV	$1s^2 2lnl' – 1s^2 2l''nl'$ $(n = 2–4)$			
	$1s^2 2lnl' – 1s^2 2l''n'l'''(n = 3, 4;\ n' = 4–8)$			
	$1s2s2p^2\ ^5\mathrm{P} – 1s2p^3\ ^5\mathrm{S}$			
UV + visible	$1s^2 2l3l' – 1s^2 2l''3l'$	Ion beams: Beam-foil	8	1969-2001
	$1s^2 2lnl' – 1s^2 2l''n'l'''$ $(n = 6–9;\ n' = 7–15)$	Astrophysical: Sun, stars, galaxies	4	1972-2004
Complementary techniques				
Auger electron spectroscopy	$1s2lnl'n'l'' \rightarrow \mathrm{Ne}^{7+}(1s^2 2s,\ 1s^2 2p) + e$ $(n = 2, 3;\ n' = 2–4)$		5	1974+1997
EBIT: Charge exchange	$\mathrm{Ne}^{7+}(1s^2 2s) + \mathrm{He} \rightarrow 1s^2 2lnl' + \mathrm{He}^+$ $(n = 3, 4)$		1	2002

levels [14–16,38] in some cases contradicts identifications of observed Auger electron peaks [32,34,35].

The purpose of the present work is to provide comprehensive and mutually consistent lists of spectral lines and energy levels of Ne VII. In order to do that, we compiled and analyzed the entire set of available experimental data on Ne VII obtained by all different methods. Consolidation of all experimental data linked together with the previous semiempirical analysis of the Be I isoelectronic sequence in the interval O V through Si XI [45] enabled us to resolve virtually all contradictions and identify a number of new lines in the line lists obtained earlier. The Ph.D. thesis of Lapierre [46] contains a complete set of moderate-resolution beam-foil spectrograms of the neon spectrum in the extreme ultraviolet (EUV) region (60–150 Å). This set of spectrograms contains all but the weakest Ne VII lines observed by Hermansdorfer [8] and Tondello and Paget [4]. It facilitated establishing a uniform scale of relative intensities of the lines in this wavelength region, as well as resolving the ambiguities in the measured wavelengths. The Ph.D. thesis of Bastin [47] provided wavelengths and intensities of several weak lines that we identified as belonging to Ne VII. Finally, we analyzed previously unpublished beam-foil spectrograms obtained by Buchet-Poulizac et al. [31] and identified several tens of new spectral lines of Ne VII. The new identifications filled in almost all gaps in the known spectrum and allowed us to construct an optimized scheme of energy levels consistent with all identified lines.

2 Observed spectral lines of Ne VII with excited n = 2 electrons

The total list of observed lines of Ne VII, from 13 Å to 3644 Å, is presented in Table I (see the *Supplementary Online Material*). In this table, the energy level classifications are given as well. These will be discussed in further sections. The observed line intensities reported by different authors were converted to a uniform scale. Below, a detailed discussion of the line classifications is given.

2.1 Review of the early studies of the Ne VII spectrum

The first observation of the resonance lines of Ne VII was made by Fawcett et al. [1] using a high-temperature discharge in neon-doped deuterium. Bockasten et al. [3] used a toroidal discharge installation to produce a high-temperature low-density plasma. They improved the measurement accuracy of the $2s^2\ ^1\mathrm{S}_0 – 2s2p\ ^1\mathrm{P}^\circ_1$ line to ±0.002 Å, and the $2s2p\ ^3\mathrm{P}^\circ – 2p^2\ ^3\mathrm{P}$ multiplet to ± 0.005 Å. In addition, Bockasten et al. identified the $2s3s\ ^3\mathrm{S}_1 – 2s3p\ ^3\mathrm{P}^\circ$ multiplet located between 1980 Å and 1998 Å. Their measurements of these lines remain the most accurate up to now. From them, Bockasten et al. deduced the energy levels of the $2s2p$ configuration and triplet levels of the $2p^2$, $2s3s$ and $2s3p$ configurations. The missing singlet states were identified later by Johnston and Kunze [6,48] and Hardis et al. [21]. The wavelength of the $2s2p\ ^1\mathrm{P}^\circ_1 – 2p^2\ ^1\mathrm{D}_2$ transition, 973.302 ±0.005 Å, was accurately measured by Lindeberg [7] in emission of a theta pinch plasma. Lindeberg also assigned another line at 562.398 Å line to the $2s2p\ ^1\mathrm{P}^\circ_1 – 2p^2\ ^1\mathrm{S}_0$ transition in Ne VII. However, this assignment must be discarded because Edlén's isoelectronic interpolation [49] yields the wavelength 561.271 ± 0.016 Å for this transition. This transition was observed and identified in a foil-excited neon beam spectrum by Hardis et al. [21]. Its wavelength, 561.25 Å, was obtained by least-squares decomposition of a blended line profile at 561.3 Å. The measurement uncertainty stated in Hardis et al. [21] was ±0.01 Å. Werner

et al. [42] recently observed the 973.302 Å line in absorption spectra of white dwarf stars. They also identified six lines in the range 3853–3912 Å belonging to the $2s3p\ ^3\mathrm{P}^\circ$–$2s3d\ ^3\mathrm{D}$ multiplet.

The connection between the singlet and triplet term systems is provided by the very weak intercombination $2s^2\ ^1\mathrm{S}_0$–$2s2p\ ^3\mathrm{P}^\circ_1$ line predicted by Edlén et al. [50] at 895.18 Å. This line was first observed in the laboratory by Tondello and Paget [4,5] and Johnston and Kunze [6]. Ridgeley and Burton [40] measured this wavelength as 895.12 ± 0.05 Å in the spectrum of the solar limb. Edlén's interpolation [49] resulted in the wavelength 895.19 ± 0.02 Å, which we adopted as the most accurate value.

The structure of the $n = 2$ complex of beryllium-like ions was studied in several papers of Edlén [49,51–53]. In reference [49], recommended values of energy levels were given for the $2s2p$ and $2p^2$ configurations. In reference [53], some correction of the $2p^2\ ^3\mathrm{P}$ levels was made, affecting the predicted values for heavier elements $Z \geq 20$. We have retained Edlén's value of the $2s2p\ ^3\mathrm{P}^\circ_1$ level (111708 ± 3 cm^{-1})[1] [49], as it is more accurate than the one derived from the 895.12 Å line discussed above. All the other levels of the $n = 2$ complex given in the present compilation are derived from the observed spectral lines with the same or slightly smaller uncertainty than Edlén's values.

The higher-lying configurations were observed in grazing incidence spectra of theta-pinch discharges, first by Fawcett et al. [2], and then, with lower uncertainties, by Tondello and Paget [4] and by Hermansdorfer [8]. Tondello and Paget used a spectrograph equipped with a 600 lines/mm, 2 m grating. The entrance slit width was 10 μm. Hermansdorfer [8] used a better grating (3600 lines/mm, 1 m) with the same entrance slit width 10 μm. The image of the entrance slit on his films had spectral width 0.03 Å. Nevertheless, the lack of proper reference lines and the use of photographic films by Hermansdorfer [8] instead of plates restricted the absolute wavelength-measurement uncertainty to ±0.05 Å, while Tondello and Paget [4] could attain an uncertainty as small as ±0.005 Å for some lines that were observed in several orders of diffraction. Fortunately, Hermansdorfer was unaware of the work of Tondello and Paget [4], so he independently measured some of the lines listed in the latter paper. Thus, the lines accurately measured in Tondello and Paget [4] can serve as secondary wavelength standards in the line list of Hermansdorfer [8]. The Ne V lines measured by Paul and Polster [55] can also be used for this purpose, since they were measured with the use of a very good equipment (3 m grazing incidence spectrograph with dispersion approximately 1 Å/mm at 500 Å and photographic plates of good quality). Comparing Hermansdorfer's wavelengths [8] with more precise ones from Tondello and Paget [4] and Paul and Polster [55] in many cases makes it possible to restrict Hermansdorfer's wavelength uncertainty to ±0.02 Å. This can be done only for the lines that are in close proximity (not farther than 0.5 Å) to the reference lines, because more distant lines could suffer from the film deformation in Hermansdorfer's spectrograph.

[1] The customary unit cm^{-1} for energy levels, used here, is related to the SI unit for energy (joule) by 1 cm^{-1} = 1.986 445 61(34)×10^{-23} J [54].

2.2 Resolution of inconsistencies in early identifications

The line assignments independently made by Hermansdorfer [8] and Tondello and Paget [4] significantly increased the number of known Ne VII lines and refined the accuracy of lines measured by Fawcett et al. [2]. However, as noted above, some of the line identifications made by Hermansdorfer [8] and Tondello and Paget [4] are inconsistent. This concerns the $n = 3$ levels determined from transitions to the $2p^2\ ^1\mathrm{S}_0$ and $^1\mathrm{D}_2$ levels. Contradiction between the identifications of the $2p3d\ ^1\mathrm{P}^\circ_1$ level in Tondello and Paget [4] and Hermansdorfer [8] was resolved by Hardis et al. [21] in favor of Hermansdorfer. The discussion in Hardis et al. [21] suggests that the wavelength 110.00 Å reported by Hermansdorfer [8] for the $2p^2\ ^1\mathrm{D}_2$–$2p3d\ ^1\mathrm{P}^\circ_1$ transition is a misprint that should read as 111.00. This suggestion is based on the fact that the value 110.00 is out of the increasing-wavelength order of the linelist of Hermansdorfer [8], and also on two closed loops formed by the (corrected) value 111.00 Å with the lines at 82.11 Å and 121.20 Å identified in reference [8]. Buchet-Poulizac et al. [31] observed this line at 111.030 ± 0.025 Å in second order of diffraction. In the spectrum observed by Hermansdorfer [8], this line was resolved from the much more intense Ne VI transition ($2s^22p\ ^2\mathrm{P}^\circ_{1/2}$–$2s2p(^3\mathrm{P}^\circ)3p\ ^2\mathrm{D}_{3/2}$ at 111.10 Å and $2s^22p\ ^2\mathrm{P}^\circ_{3/2}$–$2s2p(^3\mathrm{P}^\circ)3p\ ^2\mathrm{D}_{5/2}$ at 111.16 Å). The 111.00 Å line is seen in the first order of diffraction on the spectrogram presented in Lapierre's thesis [46] as a small shoulder on the short-wavelength side of the strong Ne VI line. The line at 111.152 ± 0.010 Å that was attributed to the $2p^2\ ^1\mathrm{D}_2$–$2p3d\ ^1\mathrm{P}^\circ_1$ transition by Tondello and Paget [4] apparently corresponds to the $2s^22p\ ^2\mathrm{P}^\circ_{3/2}$–$2s2p(^3\mathrm{P}^\circ)3p\ ^2\mathrm{D}_{5/2}$ transition in Ne VI observed at 111.16 Å by Hermansdorfer [8]. The spectrogram on which Buchet-Poulizac et al. [31] observed the 111.03 Å line was taken at a neon beam energy of 10.4 MeV. Although at such high beam energies the Ne VI intensity strongly decreases, blending was still possible. On the other hand, the good agreement between the wavelengths of the Ne VI line (111.16 [8] and 111.152 [4]) indicates that the uncertainty of the 111.00 Å measurement by Hermansdorfer [8] probably does not exceed ±0.02 Å. Therefore, we retained Hermansdorfer's value for the wavelength of this line.

The line at 121.774 Å, previously assigned to the $2p^2\ ^1\mathrm{S}_0$–$2p3d\ ^1\mathrm{P}^\circ_1$ transition by Tondello and Paget [4], is now classified as $2p^2\ ^1\mathrm{D}_2$–$2p3s\ ^1\mathrm{P}^\circ_1$, according to Hermansdorfer [8].

Another controversy between different authors concerns the $2p^2\ ^1\mathrm{S}_0$–$2p3s\ ^1\mathrm{P}^\circ_1$ transition. This transition was associated with the lines at 134.82 Å (by Fawcett

et al. [2]) or 133.64 Å (by Tondello and Paget [4]). Finally it was identified by Hermansdorfer [8] with the line at 134.12 Å, which fits well with the above-mentioned 121.774 Å line. The first of the two former candidates for this transition (134.82 Å [2]) was found to belong to Ne VI (134.83 Å [8]). The other one, observed by Tondello and Paget at 133.64 Å, remains unclassified.

In addition to the contradictions discussed above, we found a number of other inconsistencies in the line lists of Hermansdorfer [8] and Tondello and Paget [4], as well as in the new identifications [29–31]. In order to resolve them, we made parametric calculations of the Ne VII spectrum using Slater parameters and average configuration energies interpolated along the Be I isoelectronic sequence between O V and Si XI [45], employing Cowan's codes [56]. The configurations that were included in these calculations are as follows: $2sns$, $2snd$, $2sng$ ($n \leq 9$), $2pnp$, $2pnf$, ($n \leq 7$), and $2snp$, $2snf$, $2snh$, ($n \leq 9$), $2pns$, $2pnd$, and $2png$ ($n \leq 7$). Parameter values for the $2p3p$ configuration that we used were different from those published in [45], as we discovered that the irregularities in Z-dependencies of Slater parameters obtained in [45] for F VI are caused by misidentification of the $2p3p\ ^1S_0$ level by Engström [57]. The position of the F VI $2p3p\ ^1S_0$ level predicted using interpolated values of the Slater parameters is 941100 ± 500 cm^{-1}. The energy of this level given by Engström [57], 934650 cm^{-1}, deviates from the predicted value by 6450 cm^{-1}.

On the basis of these parametric calculations, some definite conclusions could readily be made, as most of the energy levels were predicted with uncertainties of less than ±1000 cm^{-1}. Revised and new classifications are detailed below by order of increasing wavelength ranges.

The classifications in the region 60 Å to 120 Å are explained in Section 2.2.1 available in the *Supplementary Online Material*.

2.3 New identifications in the EUV region (200–406 Å)

The corrections and new identifications described above significantly improved knowledge about the levels of the $n = 3$ configurations and enabled us to identify several tens of new lines in the region 200 Å through 406 Å. These new identifications were made on the spectrograms obtained in the course of work published earlier by Buchet-Poulizac et al. [31]. Although the analysis done in the latter work was confirmed in general, a few of the line assignments made therein had to be corrected. These corrections, as well as some questions regarding the new identifications, are described in detail in Section 2.3.1 available in the *Supplementary Online Material*.

2.4 New identifications in the published VUV spectra (500–900 Å)

According to our calculations with Cowan's codes, the fine-structure splitting of the $2s6g\ ^3G$ term should not exceed 12 cm^{-1}. We established the position of this term based on the new identification of a weak line seen at 534.7 ± 0.2 Å on the spectrogram presented in Figure 1 of Hardis et al. [21]. We classified this line as the unresolved $2s4f\ ^3F^\circ$–$2s6g\ ^3G$ transition array, the strongest component being due to the $J = 4$–$J = 5$ transition. The position of the $2s4f\ ^3F^\circ$–$2s6g\ ^3G$ line was obtained by linear interpolation between the positions of the peaks given in Hardis et al. [21], as well as those independently measured by Bastin [47]. The intense unidentified line on the left of the $2s4f\ ^3F^\circ$–$2s6g\ ^3G$ line (see Fig. 1 in Hardis et al. [21]) was measured at 533.42 Å in Bastin's thesis [47].

In the Ph.D. thesis of Bastin [47], emission lines of several stages of ionization of neon were observed by means of beam-foil spectroscopy in the range 450 Å through 1150 Å. The beam energies used in this work were moderate (0.8 MeV to 2.5 MeV), as this work was focused mainly on Ne IV and Ne V. However, at the highest beam energies of 2.5 MeV, several lines of Ne VII were excited with intensities sufficient to make good measurement of their wavelengths. We identified these lines (belonging to the $2s3p$–$2p3p$, $2s4f$–$2p4f$, and $2s4d$–$2s5f$ transition arrays) based on our improved values of the $n = 3$ and $n = 4$ levels and on our parametric calculations.

2.5 Transitions between Rydberg states

Lembo et al. [24] reported an observation of the $n = 7$ to $n = 8$ hydrogenic transitions excited by charge exchange of very slow Ne^{7+} ions with neutral sodium. Lembo et al. could not exactly identify the two lines observed at 3885.3 ± 0.4 Å and 3865.6 ± 0.6 Å, because in their theoretical treatment of the $2snl$ series they neglected the configuration interaction with the displaced $2pn'l'$ series, which is very significant around $n = 8$. It must be noted that the wavelengths listed by Lembo et al. [24] are in vacuum. This is verified by the exact coincidence of the measured wavelength of the $n = 10 \rightarrow n = 9$ transition in hydrogen-like Ne X with the calculated vacuum wavelength of this transition (both values are given in the first line of their Tab. I). We made Hartree-Fock calculations with Cowan's codes RCN/RCG [56] including all $2snl$ and $2pnl$ configurations ($n \leq 15$, $l \leq 14$ for both parities). On the basis of these calculations, the observed lines are identified as the unresolved $2s7i\ ^{1,3}I$–$2s8k\ ^{1,3}K^\circ$ (air wavelength 3884.2 Å) and $2s7h\ ^{1,3}H^\circ$–$2s8i\ ^{1,3}I$ (air wavelength 3864.5 Å) transitions. Singlet and triplet mixing in the $2s7i$, $2s8i$, $2s7h$, and $2s8k$ configurations is close to 50%. Thus, all components of these two blends should have comparable intensities.

In the work of Ishii et al. [28], a similar method of calculation was employed to identify an extended set of the $n = 7$–$n = 8$ lines of Ne VII observed between 3706 Å and 3884 Å in their beam-foil experiment. Their identification of the lines observed by Lembo et al. coincides with ours. Ishii et al. listed six more observed lines belonging to this transition array and included their classifications. The line intensities given in Table I (*Supplementary*

Online Material) are estimated from the picture presented by Ishii et al. [28].

In another work by Lapierre and Knystautas [29], a number of transitions between highly excited Rydberg levels of Ne VII were identified in the range 1900 Å through 4560 Å. Our analysis confirmed most of the assignments made in this work, except for a few discussed below. It should be noted that, according to a private communication from the authors of reference [29], all wavelengths given therein are in vacuum. In the present work, we converted the vacuum wavelengths above 2000 Å to standard air using the five-parameter formula by Peck and Reeder [61]. The relative intensities of the lines observed by Lapierre and Knystautas [29] were derived from the spectrograms presented therein, as well as from numerical estimates given in Lapierre's thesis [46].

The details of the classifications of transitions between the highly excited Rydberg states in the region 1900 Å to 4560 Å are given in Section 2.5.1 available in the *Supplementary Online Material*.

2.6 The n = 3–n = 3 transitions (1970–4350 Å)

Our calculations indicate that the blended line at 1979 Å, classified as the $1s2s6h\ ^4\mathrm{H}^\circ$–$1s2s7i\ ^4\mathrm{I}$ core-excited transition in Ne VIII [29], may have a significant contribution from the $2p3s\ ^3\mathrm{P}^\circ_2$–$2p3p\ ^3\mathrm{P}_2$ transition in Ne VII. We included the Ritz wavelength 1977 ±4 Å of the latter transition in Table I.

The line at 2159.3 Å was identified as the $2s3p\ ^1\mathrm{P}^\circ_1$–$2s3d\ ^1\mathrm{D}_2$ transition by Lapierre and Knystautas [29]. Our calculations support this assignment. However, the $2p3s\ ^1\mathrm{P}^\circ_1$–$2p3p\ ^1\mathrm{D}_2$ transition is predicted to occur at nearly the same wavelength, 2161 ± 4 Å, with nearly as large transition rate. It might be masked or blended by the same line. We included the Ritz wavelength of this transition in Table I. Unfortunately, this region is not covered by the spectrograms presented in references [29,46]. Therefore, we could not provide any estimate of the intensity of the 2159.3 Å line.

As explained in Section 2.5.1, we changed the original assignment of the line at 2604.2 Å ($2s6p\ ^3\mathrm{P}^\circ$–$2s7s\ ^3\mathrm{S}$ [29]) to $2p3p\ ^3\mathrm{D}_3$–$2p3d\ ^3\mathrm{D}^\circ_3$. The new assignment is supported by several other lines involving these levels observed in references [4,31].

In agreement with a number of observed lines involving the $2p3p\ ^3\mathrm{D}_2$ and $^3\mathrm{D}_3$ levels, the weak line at 2906.1 Å [29] was firmly identified as a blend of the $2p3s\ ^3\mathrm{P}^\circ_1 - 2p3p\ ^3\mathrm{D}_2$ and $2p3s\ ^3\mathrm{P}^\circ_2$–$2p3p\ ^3\mathrm{D}_3$ transitions. Although the originally suggested $n = 10$–$n = 14$ transition in Ne VIII [29] may contribute to the observed intensity of this line, the large number of combinations strongly support the new Ne VII identifications. Similar arguments support the new identification of the very weak line at 2916.1 Å, originally assigned to the $n = 8$–$n = 12$ hydrogenic transition in Ne VI [29], as the $2p3s\ ^3\mathrm{P}^\circ_0$–$2p3p\ ^3\mathrm{D}_1$ transition in Ne VII.

We identified a weak blended line seen at 3181.4 Å in Figure 2 in Lapierre and Knystautas [29] as the $2p3p\ ^1\mathrm{P}_1$–$2p3d\ ^1\mathrm{D}^\circ_2$ transition in Ne VII. The original assignment of this transition to the line at 3119.1 Å [29] does not fit with the firmly identified $2p^2\ ^1\mathrm{D}_2$–$2p3d\ ^1\mathrm{D}^\circ_2$ line at 115.955 Å [4], while the new identification fits well with this line as well as a number of other lines observed by Buchet-Poulizac et al. [31].

The line observed at 4339.5 Å by Denis et al. [9] on two spectrograms, which they found to belong to Ne VII, is now identified as the $2p3p\ ^3\mathrm{D}_3$–$2p3d\ ^3\mathrm{F}^\circ_4$ transition. This identification is in good agreement with several VUV lines involving the $2p3d\ ^3\mathrm{F}^\circ_4$ level that were observed by Buchet-Poulizac et al. [31].

Werner et al. [42], while investigating the absorption spectra of white dwarf stars, identified the lines at 3853.3 Å, 3866.8 Å, 3873.2 Å, 3894.0 Å, 3905.1 Å, and 3912.3 Å as fine-structure components of the $2s3p\ ^3\mathrm{P}^\circ$–$2s3d\ ^3\mathrm{D}$ multiplet. Three of these lines (those at 3866.8 Å, 3873.2 Å, and 3894.0 Å) were previously observed in emission by Denis et al. [9] using beam-foil spectroscopy.

2.7 Predicted lines

Kaufman and Sugar [64] listed predicted wavelengths of five parity-forbidden magnetic dipole transitions between the levels of the ground configuration. Although these lines may be important for diagnostics of low-density high-temperature plasmas, none of them has been observed as yet. We included these lines for completeness. Uncertainties of their Ritz wavelengths decreased by a factor of 3 to 6 compared to Kaufman and Sugar [64].

Majumder and Das [65] calculated the transition rate of the $2s^2\ ^1\mathrm{S}_0$–$2s2p\ ^3\mathrm{P}^\circ_2$ magnetic quadrupole transition. This transition may also be important for diagnostics of astrophysical plasmas. Although it was not observed so far, we included its predicted (Ritz) wavelength for completeness of the reference material.

2.8 Relative intensities of the lines

The relative intensities of all lines below 1000 Å were brought to approximately the same scale by using lines measured by several teams of authors [1,3,4,8,21,31,47,48]. The survey spectrograms of the region below 123 Å presented in Lapierre's thesis [46] helped us to build a continuous uniform scale in this region. Differences between excitation condition and registration equipment in different works preclude strict quantitative determination of the line intensities. Nevertheless, they provide a good qualitative estimate of relative line strengths, especially for closely located lines observed in the same source.

Most of the lines above 1000 Å were observed in beam-foil experiments [9,24,28,29]. Although these intensities strongly depend on the beam energy and other parameters of the experiment, they still can be used as a guide for estimating the intensities that can be observed in this type of light source. The intensity scale for the lines above 1000 Å measured by Bockasten et al. [3] in emission of a discharge plasma was adjusted so as to match the intensities observed by Lapierre and Knystautas [29] in the beam-foil experiment.

Similarly, the relative intensities of the absorption lines belonging to the $2s3p\ ^3\mathrm{P}^\circ$–$2s3d\ ^3\mathrm{D}$ multiplet (estimated from the spectrogram presented by Werner et al. [42]) were adjusted to match the intensities of the same lines observed in emission by Denis et al. [9]. The intensity scale of the latter work, in turn, was adjusted to match the scale of Lapierre and Knystautas [29].

The intensity adjustments were made by multiplying all intensities taken from the same source by the same factor. An exception was made for the lines listed in Bastin's thesis [47]. Intensities of these lines were corrected using the detection efficiency curve given in Bastin's thesis [47] and tied to the intensities of the strongest VUV lines at 465.221 Å, 558.610 Å, 561.368 Å, 561.728 Å, 562.992 Å, and 564.529 Å observed by Bockasten et al. [3].

In general, the intensity scale below 1000 Å was tied to the lines observed in emission of discharge plasmas. The intensity scale above 1000 Å is relevant to beam-foil excitation conditions.

3 Inner-shell excited spectrum

In addition to the spectrum discussed above, resulting from excitation of the $n = 2$ electrons, there is much interest in the inner-shell excited states of Ne^{6+}. The observed optical spectra of these states are very fragmentary, as discussed below.

Hardis et al. [21] identified the $1s2s2p^2\ ^5\mathrm{P}$–$1s2p^3\ ^5\mathrm{S}$ transition array in the range 524 Å to 528 Å and determined the fine-structure splitting of the $1s2s2p^2\ ^5\mathrm{P}$ term. The work of Lapierre and Knystautas [30] extended the known structure of the quintet level system to a total of 12 terms belonging to the $1s2p^3$, $1s2p^23s$, $1s2p^23p$, $1s2p^23d$, $1s2s2p3s$, $1s2s2p3p$, $1s2s2p3d$, and $1s2s2p4d$ configurations. Our calculations of energy structure and decay rates (for both radiation and autoionization), made with Cowan's codes [56], confirmed all identifications made by Lapierre and Knystautas [30] in their beam-foil spectrum between 74 Å and 107 Å. We established the position of the quintet level system relative to the ground state by using complementary data obtained by Auger electron spectroscopy (see below).

In several studies of the X-ray satellites of the Ne I K-alpha line, the peaks at 13.884 ± 0.005 Å (893.0 ± 0.3 eV [14,15,19]) and 13.844 ± 0.011 Å (895.6 ± 0.7 eV [14–16]) were identified as KL5 and KL6 transitions (Ne VII and Ne VIII, correspondingly). The spectral resolution achieved was not enough to resolve these peaks from each other. The two maxima were measured at different excitation conditions, so that the Ne VII or Ne VIII contributions would prevail in different cases. Such low resolution was insufficient to make a decisive conclusion about the origin of the peaks. However, the recent work by Wargelin et al. [38] on the dielectronic satellite lines in Ne VII unambiguously proved that the main contribution to the peak they observed at 13.879 ± 0.003 Å is due to the $1s^22s2p\ ^3\mathrm{P}^\circ_2$–$1s2s2p^2\ ^3\mathrm{D}_3$ transition. Our parametric calculations indicate that the 13.884 Å and 13.844 Å lines observed in ion-collision experiments [14,15,19] originate at least partially from the $1s^22p^2\ ^3\mathrm{P}$–$1s2p^3\ ^3\mathrm{S}^\circ$ and $1s^22s2p\ ^3\mathrm{P}^\circ$–$1s2s2p^2\ ^3\mathrm{P}$ transitions, respectively.

Our calculations using Cowan's codes confirmed the assignment of the weak dielectronic satellite line at 13.941 ± 0.004 Å [38] to the $1s^22s2p\ ^1\mathrm{P}^\circ_1$–$1s2s2p^2\ ^1\mathrm{D}_2$ transition. However, in contrast to the findings of Wargelin et al. [38], our calculations do not indicate any noticeable contribution to this line from the $1s^22p^2\ ^3\mathrm{P}_2$–$1s2p^3\ ^3\mathrm{D}^\circ_3$ transition. The dielectronic recombination rate, and hence the line intensity in the type of experiment of Wargelin et al. [38], is proportional to the Auger decay rate of the upper level to the ground state of the Li-like ion. Autoionization of the $1s2p^3\ ^3\mathrm{D}^\circ_3$ level to the Li-like $1s^22s\ ^2\mathrm{S}_{1/2}$ level is strongly forbidden by a combination of the parity and momentum conservation rules. Therefore, the $1s^22p^2\ ^3\mathrm{P}_2$–$1s2p^3\ ^3\mathrm{D}^\circ_3$ transition should have negligible intensity attributable to dielectronic recombination. This is confirmed by our detailed calculations.

Optical transitions originating from the levels of the $1s^23lnl'$ configurations with $n \geq 3$ were investigated experimentally and theoretically by several teams of authors. We did not include the results of these studies in the present compilation. Nevertheless, for the sake of completeness of the reference material, we provide a short review of these studies in Section 3.1 available in the *Supplementary Online Material*.

The $1s^23lnl'$ states were more successfully investigated by means of Auger electron spectroscopy as discussed in the next section.

4 Observed Auger electron lines of Ne^{6+}

Additional data about the inner-shell excited states, summarized in Table 2, were obtained by means of Auger electron spectroscopy [32–37,69]. The Auger electron spectra of multiply charged neon are very complicated and hard to interpret. If certain precautions are not undertaken, the spectrum is overloaded by a multitude of superimposed peaks originating from different charge states. This has caused much controversy in the interpretation of these spectra. Nevertheless, Bruch et al. [35] were able to make unambiguous identification of several Li-like, Be-like and B-like states. They used projectile Auger-electron spectroscopy of a highly charged neon beam passing through helium gas. These experimental conditions permitted them to excite only a limited number of states formed by single or double electron capture from helium. This made the spectrum much simpler. Comprehensive theoretical calculations were employed in order to interpret the observed spectrum. The energy resolution in this work made it possible to measure the peak energies with uncertainties better than ±0.3 eV. Similar or better accuracy was achieved in the work of Kádár et al. [34] utilizing the technique of target Auger electron spectroscopy. In this work, multiply ionized neon states were formed by passing beams of other highly charged atoms through a neutral neon gas target. The observed peaks could be assigned to definite charge states of neon by comparing

Table 2. Observed Auger electron lines of Ne VII. The calculated line energies are those derived from the optimized energy levels (see further sections).

E_{obs} (eV)	Unc. (eV)	Relative Intensity[a]	E_{calc} (eV)	Unc. (eV)[b]	E_{obs}–E_{calc} (eV)	Final state (Ne VIII)		Initial state (Ne VII)[c]			Ref.
666.88	0.10	6	666.93	0.10	–0.05	$1s^22p$	$^2P^\circ$	$1s2s^22p$	$^3P^\circ$		34
669.86	0.22	4*bl*	670.09	0.14	–0.23	$1s^22p$	$^2P^\circ$	$1s(^2S)2s2p^2(^4P)$	$^5P_1$		34
			670.17	0.14	–0.31	$1s^22p$	$^2P^\circ$	$1s(^2S)2s2p^2(^4P)$	$^5P_2$		34
			670.26	0.14	–0.40	$1s^22p$	$^2P^\circ$	$1s(^2S)2s2p^2(^4P)$	$^5P_3$		34
673.62	0.12	8				$1s^22p$	$^2P^\circ$	$1s2s^22p$	$^1P_1$		34
683.05	0.14	6	682.96	0.12	0.09	$1s^22s$	^2S	$1s2s^22p$	$^3P^\circ$		34
684.05	0.24	7	684.00	0.22	0.05	$1s^22p$	$^2P^\circ$	$1s(^2S)2s2p^2(^2D)$	^3D		34
			684.0	0.3	0.05	$1s^22p$	$^2P^\circ$	$1s(^2S)2s2p^2(^4P)$	^3P		34
685.75	0.24	10*bl*	686.11	0.15	–0.36	$1s^22s$	^2S	$1s(^2S)2s2p^2(^4P)$	$^5P_1$		34
			686.20	0.15	–0.45	$1s^22s$	^2S	$1s(^2S)2s2p^2(^4P)$	$^5P_2$		34
			686.28	0.15	–0.53	$1s^22s$	^2S	$1s(^2S)2s2p^2(^4P)$	$^5P_3$		34
690.4	0.4	5				$1s^22p$	$^2P^\circ$	$1s(^2S)2s2p^2(^2S)$	$^3S_1$	?	35
		m	692.7	0.3		$1s^22p$	$^2P^\circ$	$1s(^2S)2s2p^2(^2D)$	$^1D_2$	?	
693.95	0.12	12	693.74	0.12	0.21	$1s^22p$	$^2P^\circ$	$1s2p^3$	$^5S^\circ_2$		34
694.94	0.11	4				$1s^22p$	$^2P^\circ$	$1s(^2S)2s2p^2(^2P)$	^3P	?	34
700.0	0.4	5*bl*	700.0	0.3	0.0	$1s^22s$	^2S	$1s(^2S)2s2p^2(^4P)$	^3P		35
			700.03	0.22	0.0	$1s^22s$	^2S	$1s(^2S)2s2p^2(^2D)$	^3D		35
702.00	0.16	12				$1s^22p$	$^2P^\circ$	$1s2p^3$	$^3D^\circ$		34
		m	708.7	0.3		$1s^22s$	^2S	$1s(^2S)2s2p^2(^2D)$	$^1D_2$	?	34
709.34	0.11	9				$1s^22p$	$^2P^\circ$	$1s2p^3$	$^1D^\circ_2$	?	34

[a] Line character legends are explained in the footnote to Table I. [b] The uncertainties were determined by means of the LOPT code [77]. If this column is blank, it means that the upper or lower level of the transition is determined by this line alone. [c] A question mark after the term label means that identification of this Auger line is uncertain.

their relative intensities under excitation of the neon target by different types of projectiles. The peak energies measured by Bruch et al. [35] and Kádár et al. [34] in most cases agree with each other within the measurement uncertainties. Occasional random discrepancies between their results, as large as 0.5 eV in some cases, seem to be well explained by statistical deviations. The measurements of Kádár et al. are probably more accurate because their apparatus line width was three times less than in Bruch et al. [35]. In the works of Matthews et al. [32,69] the energy resolution was approximately the same as in Kádár et al. [34] (less than 1 eV). However, the observed peaks were not identified by the authors. Superposition of spectra originating from several charge states makes it very hard to interpret their results. Itoh et al. [33] used a zero-degree Auger electron spectroscopy of Ne^{6+} projectiles selectively produced by collisions with gas targets. Uncertainties of the energies of the measured peaks were ±0.3 eV [33]. The peak energies listed in Itoh et al. [33] are in good agreement with those given by Bruch et al. [35] and Kádár et al. [34], except for the peaks at 690.6 eV and 698.6 eV [33]. These peaks were observed by Kádár et al. at 690.06 eV and 698.98 eV, respectively, and were attributed to B-like Ne VI.

Despite the thorough analyses of the charge states responsible for the observed peaks, the identifications of the peaks given in references [33–35] in many cases disagree. At least some of the disagreements are due to the fact that neither of these teams compared the observed separations between the peaks originating from the same autoionizing states with the separations between the final states well-known from optical spectra.

Connection of the observed Auger transitions with optical spectroscopy data is illustrated in Figure 1.

As seen from Figure 1, the observation of the $1s2s2p^2\ ^5P$–$1s2p^3\ ^5S^\circ$ optical transition array by Hardis et al. [21], when combined with the identification of the Auger line at 669.86 eV as the $1s2s2p^2\ ^5P \rightarrow 1s^22p\ ^2P^\circ$ transition [34,35], permits us to unambiguously validate the $1s2p^3\ ^5S^\circ \rightarrow 1s^22p\ ^2P^\circ$ assignment of the Auger line at 693.95 eV [34].

Classifications of the other Auger electron lines is discussed in Section 4.1 available in the *Supplementary Online Material*.

All identified Auger electron lines are listed in Table 2. For each line independently measured by different authors we adopted the measurement that has the lowest uncertainty and was less affected by blending with other ionization stages. Uncertainties of the energies measured by Kádár et al. [34] are derived by combining in quadrature the statistical uncertainties given in Table V of their paper with the calibration uncertainty of 0.1 eV. We assumed

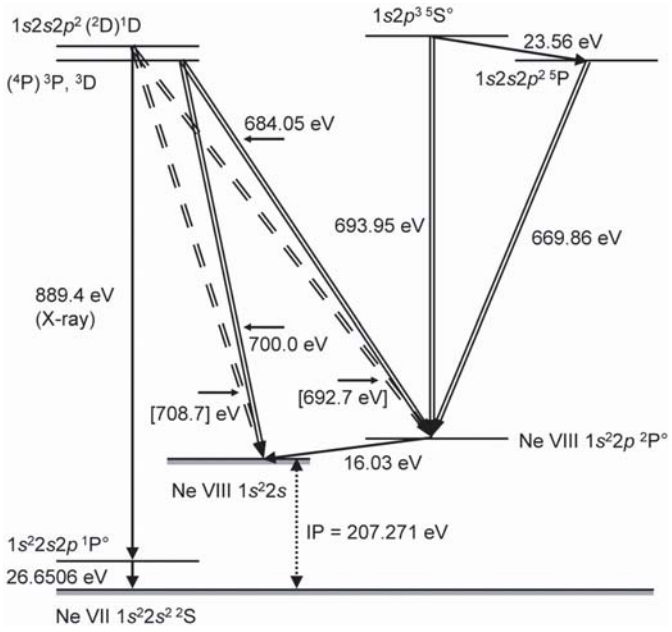

Fig. 1. Partial Grotrian diagram of the Ne VII spectrum. Optical transitions are shown as solid single-line arrows. Auger transitions to Ne VIII levels are shown as double arrows. Dashed double arrows represent predicted Auger transitions.

that the uncertainty for the blended lines is twice as large. Uncertainties of other measurements are cited from the corresponding references.

5 Energy levels of Ne VII

We derived the energy levels of Ne VII, given in Table II (see the *Supplementary Online Material*), from the observed optical spectral lines and Auger electron lines listed in Tables I and 2 by means of a least-squares optimization procedure. The computer code LOPT [77] was used for this purpose. In the process of optimization, the lowest triplet level $2s2p\ ^3P^\circ_1$ was fixed at Edlén's value 111708 ±3 cm^{-1} [49].

The conversion factor from units of eV to cm^{-1} used in the present work is 8065.54445(69) cm^{-1}/eV [54].

In the level optimization procedure, the observed energy intervals (wave numbers of the optical lines or energies of Auger lines) are weighted by factors inversely proportional to the squares of measurement uncertainties. For the components of unresolved lines, the weights were multiplied by additional factors inversely proportional to the predicted relative intensities of these components. The relative intensities of the optical lines were estimated on the basis of their transition probabilities, calculated by means of Cowan's codes [56] in an assumption that the populations of the upper levels are in local thermodynamic equilibrium. The relative intensities of the Auger electron lines are more difficult to calculate, as they are determined by the branching ratios of the Auger and radiative decays. In this work, the Auger decay rates, as well as radiative decay rates, were computed by means of Cowan's RCG code [56].

The uncertainties of the transition energies between the levels of the $n = 2$ configurations are rather small (less than ±1.6 cm^{-1}, except for the $2p^2\ ^3P_2$ and $^1S_0$ levels), while uncertainties of these levels relative to the ground state are in most cases in the range ±3 to ±4 cm^{-1}, except for the $2s2p\ ^1P^\circ_1$ and $2p^2\ ^1D_2$ levels that are known to better than ±1.5 cm^{-1}. As the $n \geq 3$ configurations lie considerably higher, they are connected to the ground state only by short-wavelength lines measured with significantly lower accuracy. Thus, their uncertainty is much larger. With few exceptions, it is between ±40 cm^{-1} and ±130 cm^{-1} for all the $n = 3$ levels as well as for the $2s4l$ levels, and ±60 cm^{-1} to ±500 cm^{-1} for higher levels. Some of the levels, e.g. $2s5d\ ^3D_1$, $2s6p\ ^1P^\circ_1$, $2p4d\ ^3F^\circ_4$, $2p5d\ ^3F^\circ_2$, and $2s9d\ ^3D$, are determined from poorly measured or blended lines. They have uncertainties as large as ±900 cm^{-1}.

The inner-shell excited levels derived from the Auger electron lines or X-ray spectra are expected to have uncertainties in the range ±900 cm^{-1} to ±3000 cm^{-1}, except for $1s2p^3\ ^3P^\circ$ and $^3S^\circ$, which have uncertainties ±4000 cm^{-1} and ±12000 cm^{-1}, respectively.

The quintet inner-shell excited states are connected to the $1s^22s$ Ne VIII ground state by means of Auger electron lines observed at 669.86 ± 0.22 eV, 685.75 ± 0.24 eV, and 693.95 ± 0.12 eV [32,34,35] (see Fig. 1). The unknown shift x of the quintet system relative to the ground state of Ne VII is determined by the uncertainties of these lines and is estimated to be not greater than ±1100 cm^{-1}. Theoretical calculations of the energies of the quintet states [78,79] could not provide better accuracy.

The wavelengths of the transitions making main contributions to the above-mentioned X-ray line at 13.884 Å, which are due to the radiative decay of the $1s(2s2p^2\ ^4P)\ ^3P$ and ^3D states, can be accurately predicted on the basis of the optimized energy levels (see the column of calculated wavelengths in Tab. I).

The question marks after certain level energies in Table II indicate that identifications of transitions determining this level are doubtful. These include $1s^22s5s\ ^1S_0$, $1s^22s6p\ ^3P^\circ_1$, $1s^22s7s\ ^3S_1$, $1s^22s8f\ ^1F^\circ_3$, $1s^22s8f\ ^3F^\circ$, and $1s^22p5f\ ^3D_{2,3}$, as well as the inner-shell excited $1s2s2p^2\ ^3S_1$, $1s(2s2p^2\ ^2P)\ ^3P$, $1s2p^3\ ^1D^\circ_2$, $1s2p^3\ ^3P^\circ$, and $1s2p^23p\ ^5S^\circ_2$ levels for which the identifications of the corresponding Auger electron or optical lines are uncertain.

The percentage composition of the levels in Table II was computed by means of the parametric fitting using Cowan's RCE code [56]. As described above, the parameter values scaled along the Be I isoelectronic sequence in the interval between O V and Si XI [45] resulted in an average deviation of calculated levels from experimental ones as low as 500 cm^{-1}. Fitting with updated level values reduced the level deviations to 250 cm^{-1} and 360 cm^{-1} for even and odd configurations, respectively, and altered the parameters by reasonably small amounts.

Configuration and term labels of several highly mixed levels have little physical meaning. In most cases they

are chosen based on the leading component of the level character in LS coupling scheme. The only exception is the $1s^2 2p5d\ ^3P^\circ_2$ level for which the leading component is 47% of $^3D^\circ_2$. This level was labeled based on the energy separations between calculated positions of the levels belonging to the $1s^2 2p5d\ ^3P^\circ$ and $^3D^\circ$ terms. The $2p4d\ ^3F^\circ$ and $2s5f\ ^3F^\circ$ levels are strongly mixed. Although the labels that we chose for them are rather arbitrary, all of them represent the component that has more than 50% of the level composition as obtained with the parametric fitting. The levels at 1458419 cm^{-1} and 1458703 cm^{-1}, denoted in Table II as $2s5f\ ^3F^\circ_3$ and $^3F^\circ_4$, are the same as those denoted by Buchet-Poulizac et al. [31] as $2p4d\ ^3F^\circ_3$ and $^3F^\circ_4$, respectively. The small energy separations within the terms support our naming convention.

The recent work of Fischer et al. [39] introduced a novel experimental technique for analyzing the atomic energy structure. A monoenergetic beam of Ne^{7+} ions extracted from EBIT was passed through a cold beam of He atoms, where a single-electron charge exchange occurred. The recoil He^+ ions were extracted along the projectile beam and accelerated using a small calibrated electric field. Their energy spectrum was measured with high resolution. The momentum of the recoil ions depends linearly on the difference of binding energies of the initial and final projectile states. Hence, measurement of this momentum provides for a unique method to directly measure the structure of moderately excited non-autoionizing energy levels of the resulting Ne^{6+} ion. Extracting the energy levels from the recoil-momentum data requires only the knowledge of the ionization potential of Ne^{6+}. The energy resolution of 0.7 eV achieved in the work of Fischer et al. [39] still cannot compare with the accuracy of optical measurements. Nevertheless, their results provide a good independent test for the identifications made in the optical studies. In particular, they support the identifications of the $2s4f$ levels by Buchet-Poulizac et al. [31], as well as the new identifications made in the present work.

For the sake of completeness of the reference material, we mention that radiative lifetimes of several non-autoionizing states were measured by means of beam-foil spectroscopy [11–13,20,26], and the mean lives of the metastable $1s(2s2p^2\ ^4P)\ ^5P$ (J = 2, 3) levels were measured by Schumann et al. [80] by means of registration of delayed Auger decay spectra excited by passing an ion beam through a foil. Optical spectroscopy also yielded measurements of lifetimes of several core-excited states. The lifetime of the $1s2p^3\ ^5S^\circ_2$ level was measured by Hardis et al. [21]. Lapierre and Knystautas [30] measured the lifetimes of three higher-lying quintet terms, $1s2s2p3s\ ^5P^\circ$, $1s2s2p3d\ ^5D^\circ$, and $1s2s2p4f\ ^5F$.

6 Ionization potential

In this section we will analyze the available experimental and theoretical data on the ionization potential (IP) of Ne VII and then select the best value based on this comparison.

6.1 Experimental data

Prior to this work, the longest Rydberg series observed experimentally in the Ne VII spectrum were $2snd\ ^1D$ ($n \leq 7$) and $2snd\ ^3D$ ($n \leq 8$). These series are strongly perturbed at $n = 3$ by $2p3p\ ^{1,3}D$, at $n = 5$ by $2p4p\ ^{1,3}D$, and at $n = 8$ by $2p5f\ ^{1,3}D$. In addition, the $2s5d\ ^1D$ and $2s5d\ ^3D$ terms were missing (see discussion in Sect. 2 regarding the 80.533 Å and 74.40 Å lines). The position of the $2s7d\ ^3D$ and $2s8d\ ^3D$ terms was very uncertain because of blending of the corresponding lines in the VUV region. For these reasons, prior to the present work, the ionization potential (IP) of Ne VII could be derived from the observed lines only with a relatively low accuracy (1672000 ± 1000 cm^{-1} [4]).

The identifications made in the present work allowed us to establish the excitation energies of several highly-excited hydrogenic levels up to $n = 15$ with uncertainties as low as 80 cm^{-1} relative to the ground state. It should be noted that the $2snf$, $2sng$, and $2snh$ series are strongly perturbed by the displaced $2pn'd$, $2pn'f$, and $2pn'g$ series, correspondingly. This makes it difficult to apply the polarization formula to the calculation of these series. While fitting the polarization formula, we excluded the strongly perturbed $2s5g$, $2s8f$, $2s8g$, and $2s8h$ configurations from the fit. The weights of the less strongly perturbed $2s5f$, $2s6f$, and $2s7f$ configurations were decreased to 0.3, 0.2, and 0.1, respectively. The weights of all the other included configurations, i.e. $2s4f$, $2s6g$, $2s6h$, $2s7g$, $2s7h$, $2s7i$, $2s8i$, $2s8k$, $2s9g$, $2s9h$, $2s9k$, $2s10l$, $2s11l$, $2s12l$, $2s13m$, $2s14m$, and $2s15m$ were taken to be equal to 100 divided by the uncertainty of the average energy of each of these configurations relative to the ground state (see Tab. II). The resulting value of the first ionization limit is 1671900 ± 100 cm^{-1}. This value should be compared with theoretical and semi-empirical results discussed below.

6.2 Theoretical data

Lotz [81] used interpolation of the difference between the IP of Be-like and Li-like ions along the isoelectronic sequence to obtain the value 1671640 cm^{-1}. Edlén [58,59], using a theoretically derived Z-dependence of the IP with an empirical relativistic correction extrapolated from the interval Be I through O V, obtained the value 1671792 cm^{-1} cited by Moore [82] and Kelly [44]. Odabasi [83] tried to improve Edlén's extrapolation by the use of a theoretical relativistic correction and obtained 1671821 cm^{-1}.

A number of theoretical studies were devoted to the problem of calculation of the IP of Be-like systems. Davidson et al. [84] reported the value 1669877 cm^{-1} resulting from their non-relativistic multiconfiguration Hartree-Fock calculations with stationary nucleus. Chung et al. [85] used a saddle-point technique with an account for quantum-electrodynamic (QED) and relativistic corrections and obtained 1671744.6 cm^{-1}. Safronova and Shlyaptseva [86] obtained 1671970 cm^{-1} by the use of the

$1/Z$-expansion approach that includes QED and relativistic corrections. Chen and Cheng [87] reported the IP of Ne VII to be 1671725.3 cm^{-1} obtained by means of a large-scale relativistic configuration-interaction calculation.

The quality of different theoretical and semiempirical calculations can be estimated on a test case of F VI, where an accurate measurement of Engström is available [53]. Engström's value of the IP of F VI is 1267606 ± 2 cm^{-1}. Edlén's extrapolation yields 1267622 cm^{-1}. The good agreement between Edlén's extrapolation and experimental data leads to the conclusion that the uncertainty of his value for Ne VII is about ±100 cm^{-1}. Chung et al. [85] report 1267606.7 cm^{-1} for F VI, while the results of the other authors deviate more from Engström's value: 1267635.0 [83], 1266516 [84] (non-relativistic, stationary nucleus approximation), and 1267800 cm^{-1} [86]. Chen and Cheng [87] presented the IP values only for $Z = 10, 15$ and 20, so we cannot test their accuracy in this way. Another test is provided by comparing the calculated excitation energies of the $2s2p\ ^1P_1^\circ$ and $^3P_1^\circ$ levels from Chung et al. [85] and Chen and Cheng [87] with the experimental energies (214951.6 ±1.3 cm^{-1} and 111708 ± 3 cm^{-1}, respectively, see Tab. II). The energies given by Chung et al. [85] deviate from the experimental energies by +35 cm^{-1} and –12 cm^{-1}, while those of Chen and Cheng [87] deviate by +68 cm^{-1} and +12 cm^{-1}, respectively. Chung et al. [85] actually calculated the double-ionization potential, that is, the energy difference between the $1s^2$ ground state of He-like neon and the $1s^22s^2$ ground state of Be-like neon. From this value they subtracted Chung's previously published theoretical ionization potential of Li-like neon [88,89]. According to the work by Chen et al. [90], Chung's result [88,89] for Li-like Ne^{7+} may be in error by approximately 10 cm^{-1} due to the omission of higher-order relativistic corrections. An additional source of error is the uncertainty of the calculated quantum electrodynamics corrections. The controversy between different authors about the value of these corrections indicates that its uncertainty in Chung's calculations [89] is as large as ±30 cm^{-1} for Ne^{7+}. Since his value of the IP of the Li-like ion makes a large contribution to the result of Chung et al. [85] for the IP of the Be-like ion, the latter is uncertain to at least ±40 cm^{-1}. Thus, the coincidence of the results of Chung et al. [85] with Engström's experimental IP of Be-like F^{5+} should be treated as accidental. In addition, the recent benchmark calculations by Komasa [91] have lowered the upper bound of the non-relativistic energy of the Ne^{6+} ground state by approximately 108 cm^{-1} compared to the value calculated by Chung et al. [85]. These considerations result in a conclusion that even the most extensive theoretical calculations do not provide accuracy better than that of Edlén's extrapolation.

Biémont et al. [92] systematically investigated the behavior of the differences between experimental values of IPs and those calculated ab initio by means of multiconfigurational Dirac-Fock approach along isoelectronic sequences. Their interpolated value for Ne VII is 1671600 ± 80 cm^{-1}.

6.3 The adopted value of the IP

Summarizing the preceding analysis, there are three accurate results for the IP of Ne VII having well-defined uncertainties: the value given above from Biémont et al. [92], 1671600 ± 80 cm^{-1}, Edlén's value 1671792 ± 100 cm^{-1}, and the present experimental value derived from high hydrogenic levels, 1671900 ± 100 cm^{-1}. We adopted the weighted average of these three values, 1671750±100 cm^{-1} (207.271±0.013 eV), as the best value for the IP of Ne VII.

7 Conclusion

In the course of the present work, the entire set of consolidated experimental data, including previously unpublished ones, was critically evaluated and analyzed. As a result, mutually consistent tables of energy levels, wavelengths of spectral lines, and energies of Auger transitions were built. The level list includes 200 energy levels, of which approximately half were newly identified in this work. Most of the others have significantly decreased uncertainties compared to earlier data. The line list includes approximately 350 transitions, almost half of which were newly identified in this work. For 40 transitions, the previous identifications were revised. On the basis of the new identifications, energies of several highly excited hydrogenic configurations were determined with uncertainties 80 cm^{-1} to 100 cm^{-1}. This enabled us to derive a new value of the ionization potential of Ne VII with improved confidence.

The authors are grateful to A. Lapierre and T. Bastin for making their Ph.D. theses available and for helpful communication. This work was supported in part by the Office of Fusion Energy Sciences of the U.S. Department of Energy and by National Aeronautics and Space Administration.

References

1. B.C. Fawcett, B.B. Jones, R. Wilson, Proc. Phys. Soc. **78**, 1223 (1961)
2. B.C. Fawcett, A.H. Gabriel, B.B. Jones, N.J. Peacock, Proc. Phys. Soc. **84**, 257 (1964)
3. K. Bockasten, R. Hallin, T.P. Huges, Proc. Phys. Soc. **81**, 522 (1963)
4. G. Tondello, T.M. Paget, J. Phys. B **3**, 1757 (1970)
5. G. Tondello, R.W.P. McWhirter, J. Phys. B **4**, 715 (1971)
6. W.D. Johnston III, H.-J. Kunze, Phys. Rev. A **4**, 962 (1971)
7. S. Lindeberg, *An Experimental Analysis of the Energy Levels with n = 2 in the Spectra Ne IV, V, VI and VII*, Uppsala Univ. Inst. Phys., Report UUIP-759, 1 (1972)
8. H. Hermansdorfer, J. Opt. Soc. Am. **62**, 1149 (1972)
9. A. Denis, J. Désesquelles, M. Dufay, J. Opt. Soc. Am. **59**, 976 (1969)
10. A. Denis, J. Désesquelles, M. Dufay, Compt. Rend. Acad. Sci. B **272**, 789 (1971)
11. G. Beauchemin, J.A. Kernahan, É.J. Knystautas, D.J.G. Irwin, R. Drouin, Phys. Lett. A **40**, 194 (1972)

12. D.J.G. Irwin, A.E. Livingston, J.A. Kernahan, Can. J. Phys. **51**, 1948 (1973)
13. L. Barrette, R. Drouin, Phys. Scripta **10**, 213 (1974)
14. C.F. Moore, J.E. Bolger, K. Roberts, D.K. Olsen, B.M. Johnson, J.J. Mackey, L.E. Smith, D.L. Matthews, J. Phys. B **7**, L415 (1974)
15. D.L. Matthews, B.M. Johnson, C.F. Moore, Phys. Rev. A **10**, 451 (1974)
16. D.L. Matthews, B.M. Johnson, G.W. Hoffmann, C.F. Moore, Phys. Lett. A **49**, 195 (1974)
17. L. Barrette, D.J.G. Irwin, R. Drouin, Phys. Scripta **12**, 113 (1975)
18. J.P. Buchet, A. Denis, J. Désesquelles, M. Druetta, J.L. Subtil, Beam-Foil Spectroscopy of High Ionised C, N, O and Ne Atoms at 1 MeV/Nucleon, in *Beam-Foil Spectroscopy*, Proc. 4th Int. Conf. Beam-Foil Spectrosc., Sept. 15–19, 1975, Gatlinburg, Tennessee, edited by I.A. Sellin, D.J. Pegg (Plenum Press, New York, 1976), p. 355
19. R.L. Watson, O. Benka, K. Parthasaradhi, R.J. Maurer, J.M. Sanders, J. Phys. B **16**, 835 (1983)
20. J.E. Hardis, L.J. Curtis, P.S. Ramanujam, A.E. Livingston, R.I. Brooks, Phys. Rev. A **27**, 257 (1983)
21. J.E. Hardis, H.G. Berry, L.J. Curtis, A.E. Livingston, Phys. Scripta **30**, 189 (1984)
22. M. Cornille, J. Dubau, F. Bely-Dubau, S.L. Bliman, D. Hitz, M. Mayo, J.J. Bonnet, M. Bonnefoy, M. Chassevent, A. Fleury, J. Phys. B **19**, L393 (1986)
23. M. Cornille, J. Dubau, F. Bely-Dubau, S.L. Bliman, C.-A. Laberge, É.J. Knystautas, J. Phys. B **20**, L623 (1987)
24. L.J. Lembo, K. Danzmann, C. Stoller, W.E. Meyerhof, T.W. Hansch, Phys. Rev. A **37**, 1141 (1988); L.J. Lembo, Ch. Stoller, K. Danzmann, W.E. Meyerhof, T.W. Hansch, R. Gerson, Nucl. Inst. Meth. Phys. Res. B **23**, 101 (1987)
25. S.L. Bliman, M. Cornille, É.J. Knystautas, Beam foil spectroscopic identifications of some doubly excited levels of Ne^{6+} ($2l2l'n''l''$) ^{3}L, in *UV and X-ray Spectroscopy of Astrophysical and Laboratory Plasmas* (Universal Academy Press, Inc., 1996), p. 479
26. S.L. Bliman, M. Cornille, A. Langereis, J. Nordgren, R. Bruch, R.A. Phaneuf, J. Swenson, D. Schneider, Rev. Sci. Instrum. **68**, 1080 (1997)
27. A. Langereis, J. Nordgren, R. Bruch, R. Phaneuf, S. Bliman, M. Cornille, D. Schneider, Phys. Scripta **T73**, 85 (1997)
28. K. Ishii, T. Nishida, Y. Kimura, M. Fujiwara, T. Nakano, S. Kawae, Phys. Scripta **T73**, 73 (1997)
29. A. Lapierre, É.J. Knystautas, Phys. Scripta **59**, 426 (1999) All wavelengths in this paper are reported in vacuum. Wavelengths greater than 2000 Å have been converted to standard air for the present compilation
30. A. Lapierre, É.J. Knystautas, J. Phys. B **33**, 2245 (2000)
31. M.-C. Buchet-Poulizac, P.O. Bogdanovich, É.J. Knystautas, J. Phys. B **34**, 233 (2001)
32. D.L. Matthews, B.M. Johnson, J.J. Mackey, L.E. Smith, W. Hodge, C.F. Moore, Phys. Rev. A **10**, 1177 (1974)
33. A. Itoh, D. Schneider, T. Schneider, T.J.M. Zouros, G. Nolte, G. Schiwietz, W. Zeitz, N. Stolterfoht, Phys. Rev. A **31**, 684 (1985)
34. I. Kádár, S. Ricz, J. Végh, D. Varga, D. Berényi, Phys. Rev. A **41**, 3518 (1990)
35. R. Bruch, D. Schneider, M.H. Chen, K.T. Chung, B.F. Davis, Phys. Rev. A **44**, 5659 (1991)
36. A. Bordenave-Montesquieu, P. Moretto-Capelle, D. Bordenave-Montesquieu, Phys. Scripta **T80**, 372 (1999)
37. A. Bordenave-Montesquieu, P. Moretto-Capelle, D. Bordenave-Montesquieu, J. Phys. B **36**, 47 (2003); A. Bordenave-Montesquieu, P. Moretto-Capelle, D. Bordenave-Montesquieu, J. Phys. B **36**, 65 (2003)
38. B.J. Wargelin, S.M. Kahn, P. Beiersdorfer, Phys. Rev. A **63**, 022710 (2001)
39. D. Fischer, B. Feuerstein, R.D. DuBois, R. Moshammer, J.R. Crespo López-Urrutia, I. Draganic, H. Lörch, A.N. Perumal, J. Ullrich, J. Phys. B **35,** 1369 (2002)
40. A. Ridgeley, W.M. Burton, Solar Phys. **27**, 280 (1972)
41. W.E. Behring, L. Cohen, U. Feldman, G.A. Doschek, Astrophys. J. **203**, 521 (1976)
42. K. Werner, T. Rauch, E. Reiff, J.W. Kruk, R. Napiwotzki, Astron. Astrophys. **427**, 685 (2004)
43. W.A. Feibelman, Publ. Astron. Soc. Pacific **107**, 531 (1995)
44. R.L. Kelly, J. Phys. Chem. Ref. Data Suppl. **16**, 149 (1987)
45. A.E. Kramida, E. Träbert, Phys. Scripta **51**, 209 (1995)
46. A. Lapierre, Ph.D. thesis, Laval University, Canada, 2000
47. T. Bastin, Ph.D. thesis, Liége University, France, 1996
48. W.D. Johnston III, H.-J. Kunze, Astrophys. J. **157**, 1469 (1969)
49. B. Edlén, Phys. Scripta **28**, 51 (1983)
50. B. Edlén, H.P. Palenius, K. Bockasten, R. Hallin, J. Bromander, Solar Phys. **9**, 432 (1969)
51. B. Edlén, Phys. Scripta **20**, 129 (1979)
52. B. Edlén, Phys. Scripta **22**, 593 (1980)
53. B. Edlén, Phys. Scripta **32**, 86 (1985)
54. P.J. Mohr, B.N. Taylor, *The 2002 CODATA Recommended Values of the Fundamental Physical Constants, Web Version 4.0*, available at `http://physics.nist.gov/constants` (National Institute of Standards and Technology, Gaithersburg, MD 20899, 9 December 2003); P.J. Mohr, B.N. Taylor, Rev. Mod. Phys. **77**, 1 (2005)
55. F.W. Paul, H.D. Polster, Phys. Rev. **59**, 424 (1941)
56. R.D. Cowan, *The Theory of Atomic Structure and Spectra* (University of California Press, Berkeley, 1981)
57. L. Engström, Phys. Scripta **31**, 379 (1985)
58. B. Edlén, Ionization Potentials of Atoms and Ions Containing One to Ten Electrons, in *Topics in Modern Physics - A Tribute to Edward U. Condon*, edited by W.E. Brittin, H. Odabasi (Colorado Assoc. Univ. Press, Boulder, Colorado, 1971), p. 133
59. B. Edlén, Phys. Rev. Lett. **28**, 943 (1972)
60. A.E. Kramida, M.-C. Buchet-Poulizac, *Energy levels and wavelength of Ne VIII*, Eur. Phys. J. D (to be published)
61. E.R. Peck, K. Reeder, J. Opt. Soc. Am. **62**, 958 (1972)
62. A.E. Kramida, T. Bastin, E. Biémont, P.-D. Dumont, H.-P. Garnir, J. Opt. Soc. Am. B **16**, 1966 (1999)
63. A.E. Kramida, T. Bastin, E. Biémont, P.-D. Dumont, H.-P. Garnir, Eur. Phys. J. D **7**, 547 (1999)
64. V. Kaufman, J. Sugar, J. Phys. Chem. Ref. Data **15**, 321 (1986)
65. S. Majumder, B.P. Das, Phys. Rev. A **62**, 042508 (2000)
66. J.P. Buchet, Ph.D. thesis, Univ. Claude Bernard, Lyon, France, 1976.
67. K.X. To, É.J. Knystautas, R. Drouin, H.G. Berry, J. Phys. Colloq. **40**, C1-3 (1979)
68. A.E. Kramida, I.A. Ivanov, Phys. Scripta **56**, 264 (1997)

69. D.L. Matthews, B.M. Johnson, J.J. Mackey, C.F. Moore, Phys. Rev. Lett. **31**, 1331 (1973)
70. F. Martin, O. Mo, A. Riera, M. Yanez, Phys. Rev. A **38**, 1094 (1988)
71. N. Vaeck, J.E. Hansen, J. Phys. B **22**, 3137 (1989)
72. Z. Chen, C.D. Lin, J. Phys. B **22**, 2875 (1989)
73. M. Boudjema, M. Cornille, J. Dubau, P. Moretto-Capelle, A. Bordenave-Montesquieu, P. Benoit-Cattin, A. Gleizes, J. Phys. B **24**, 1713 (1991)
74. M. Mack, A. Niehaus, Nucl. Instr. Meth. B **23**, 116 (1987)
75. M. Mack, J.H. Nijland, P. van der Straten, A. Niehaus, R. Morgenstern, Phys. Rev. A **39**, 3846 (1989)
76. P. van der Straten, R. Morgenstern, J. Phys. B **19**, (1986); P. van der Straten, R. Morgenstern, Phys. Rev. A **34**, 4482 (1986)
77. A.E. Kramida, G. Nave, Eur. J. Phys. D **37**, 1 (2006)
78. T. Brage, C. Froese Fischer, J. Phys. B **21**, 2563 (1988)
79. K.T. Chung, Phys. Rev. A **40**, 4203 (1989)
80. S. Schumann, K.-O. Groeneveld, G. Nolte, B. Fricke, Z. Phys. A **289**, 245 (1979)
81. W. Lotz, J. Opt. Soc. Am. **57**, 873 (1967)
82. C.E. Moore, *Atomic Energy Levels*, U.S.N.B.S., Circ. 467, Vol. I (1949), Vol. II (1952), Vol. III (1958)
83. H. Odabasi, Phys. Scripta **19**, 313 (1979)
84. E.R. Davidson, S.A. Hagstrom, S.J. Chakravorty, Phys. Rev. A **44**, 7071 (1991)
85. K.T. Chung, X.-W. Zhu, Z.-W. Wang, Phys. Rev. A **47**, 1740 (1993)
86. U.I. Safronova, A.S. Shlyaptseva, Phys. Scripta **54**, 254 (1996)
87. M.H. Chen, K.T. Cheng, Phys. Rev. A **55**, 166 (1997)
88. K.T. Chung, Phys. Rev. A **44**, 5421 (1991)
89. K.T. Chung, Phys. Rev. A **45**, 7766 (1992)
90. M.H. Chen, K.T. Cheng, W.R. Johnson, J. Sapirstein, Phys. Rev. A **52**, 266 (1995)
91. J. Komasa, J. Rychlewski, K. Jankowski, Phys. Rev. A **65**, 042507 (2002)
92. E. Biémont, Y. Frémat, P. Quinet, At. Data. Nucl. Data Tables **71**, 117 (1999)